Microstructure effects for Casimir forces in chiral metamaterials

Alexander P. McCauley,[1] Rongkuo Zhao,[2] M. T. Homer Reid,[1] Alejandro W. Rodriguez,[1] Jiangfeng Zhou,[3] F. S. S. Rosa,[4] John D. Joannopoulos,[1] D. A. R. Dalvit,[4] Costas M. Soukoulis,[2] and Steven G. Johnson[5]
[1]*Department of Physics, Massachusetts Institute of Technology, Cambridge, Massachusetts 02139, USA*
[2]*Ames Laboratory and Department of Physics and Astronomy, Iowa State University, Ames, Iowa 50011, USA*
[3]*MPA-CINT, Los Alamos National Laboratory, MS K771, Los Alamos, New Mexico 87545, USA*
[4]*Theoretical Division, Los Alamos National Laboratory, MS B213, Los Alamos, New Mexico 87545, USA*
[5]*Department of Mathematics, Massachusetts Institute of Technology, Cambridge, Massachusetts 02139, USA*
(Received 13 September 2010; published 6 October 2010)

We examine a recent prediction for the chirality dependence of the Casimir force in chiral metamaterials by numerical computation of the forces between the exact microstructures, rather than homogeneous approximations. Although repulsion in the metamaterial regime is rigorously impossible, it is unknown whether a reduction in the attractive force can be achieved through suitable material engineering. We compute the exact force for a chiral bent-cross pattern, as well as forces for an idealized "omega"-particle medium in the dilute approximation and identify the effects of structural inhomogeneity (i.e., proximity forces and anisotropy). We find that these microstructure effects dominate the force for separations where chirality was predicted to have a strong influence. At separations where the homogeneous approximation is valid, in even the most ideal circumstances the effects of chirality are less than 10^{-4} of the total force, making them virtually undetectable in experiments.

DOI: 10.1103/PhysRevB.82.165108 PACS number(s): 81.05.Xj, 42.50.Lc, 12.20.Ds, 42.50.Ct

I. INTRODUCTION

It has been proposed that dielectric metamaterials might exhibit repulsive Casimir forces in vacuum where planar structures have only attraction.[1–3] However, these predictions used effective-medium approximations (EMAs) for the metamaterials, often treating the EMA terms as free parameters. While certain effective-medium parameters give repulsion, these are known to be physically impossible based on causality/passivity arguments.[4] Furthermore, when the constituent materials are restricted to have unit magnetic permeability (as is common at frequencies relevant for Casimir measurements), a recent theorem[5] implies that one cannot have repulsion in the effective-medium (large-separation) regime when the materials are vacuum-separated (although repulsion is possible outside of this regime[6]). However, it is still possible that significant reduction or modulation of the Casimir force can occur as a result of metamaterial effects. A recent EMA analysis of chiral metamaterials[7] implies such a force reduction, and even repulsion, due to chirality. Unfortunately, chirality effects vanish at large separations where the EMA should be valid and are strongest at small separations where the EMA is questionable. Therefore, the question of whether chiral metamaterial effects can significantly reduce the Casimir force, at least in theory, remains open. Answering this question requires accurate calculations using the exact microstructure of the metamaterials, rather than a homogeneous EMA. Recent advances[8–14] have made the treatment of such complex structures possible. In this paper, we apply these methods to rigorously test the EMA predictions for chiral metamaterials against numerical calculations incorporating the microstructures. We are able to distinguish chiral metamaterial effects from other "nonideal" effects such as pairwise surface-surface attractions and find that the former are overwhelmed except at large separations, where they are only 10^{-4} or less of the total force. After providing background and definitions in Sec. II, we examine the force between two media composed of chiral bent-arm crosses in Sec. III. We then examine a more "ideal" isotropic chiral medium in Sec. IV. We conclude that while there is a regime in which the chiral metamaterial viewpoint does give correct predictions of the Casimir force, the effect is virtually undetectable.

II. BACKGROUND AND DEFINITIONS

Dielectric and metallic metamaterials are defined by an inhomogeneous permittivity $\varepsilon(\mathbf{x},\omega)$, but at sufficiently long wavelengths (large separations in the Casimir context) they can be accurately modeled in the EMA by homogeneous constitutive parameters [e.g., $\varepsilon(\omega)$, $\mu(\omega)$] that can be very different from the constituent materials. The Casimir force between two bodies, however, is naturally expressed as an integral over imaginary frequency $\omega=i\xi$.[15] The force in the EMA will then depend on the effective $\varepsilon(i\xi)$, $\mu(i\xi)$, etc., over a range of imaginary frequencies.[3] Early works[1,2,16] predicted repulsive effects by a putative $\varepsilon(i\xi)<\mu(i\xi)$ for one body. However, no such repulsion was found for "magnetic" metamaterials based on actual structures, in which $\varepsilon(i\xi)>\mu(i\xi)$ for all ξ.[3,17] Basically, while these metamaterials can have almost any ε and μ at a given *real* ω via resonances, on the imaginary-ω axis the important features come from the behavior at low ξ (long wavelengths). In this limit, $\mu(i\xi)-\mu(0)\sim-\xi^2$,[3,17,18] where $\mu(0)<\varepsilon(0)$. Therefore, there is no repulsion or force reduction in the EMA regime for this model. More recently, Ref. 7 studied chiral metamaterials, which in addition to ε and μ are characterized in the EMA by a chirality κ coupling $\mathbf{D}$ to $\mathbf{H}$ and $\mathbf{B}$ to $\mathbf{E}$. $\kappa\to-\kappa$ by a spatial inversion $(\mathbf{x}\to-\mathbf{x})$ of the microstructure. For any κ, the EMA predicts that the force between two media of the

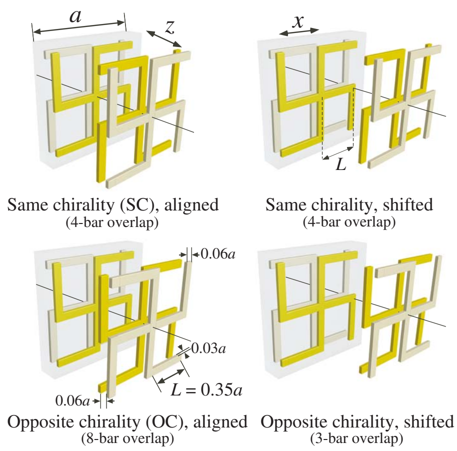

FIG. 1. (Color online) Interactions between two chiral metamaterials (Ref. 20). Shaded box indicates a unit cell; the structures are periodic in the transverse direction. Nearest-neighbor bars on opposing structures are shaded yellow. In the EMA, the forces should obey $F_{SC}<F_{OC}$. By contrast, in the pairwise-force approximation the force is determined by the number of overlapping nearest-neighbor bars, as indicated: $F_{OC}>F_{SC}$ when the centers are aligned (left column) but $F_{OC}<F_{SC}$ when they are displaced by $L/2$ (right column).

same chirality (SC) should be lower than for media of the opposite chirality (OC) with the size of this difference increasing with κ. Because, in general, $\kappa\sim\xi$,[7,18] this effect is largest at short separations and goes to zero at large separations. Therefore, to get a useful prediction (e.g., force reduction due to chirality), we are forced to consider the predictions of the EMA at intermediate separations. However, not only does the EMA fail at sufficiently small separations but the force in that limit is eventually described by the proximity force approximation (PFA)[19] in which there are only pairwise attractions. One should therefore be cautious of any EMA prediction that differs qualitatively from PFA in this limit. An analysis based on pairwise attractions would find little effect due to chirality. Instead, the behavior would be dominated by small-scale features such as the shortest distance between two components of the microstructures. Thus far, no attempt has been made to determine which behavior dominates, and we do this as follows: if the materials behave as homogeneous, chiral media, the relative chirality should be the only source of a force difference between the SC and OC cases, where $F_{OC}>F_{SC}$, independent of the transverse displacement x. However, if the force is governed by pairwise attraction, it should exhibit a strong x dependence. We can therefore directly test the validity of the EMA by comparing the force for different values of x.

III. BENT-ARM CROSSES

We first examine a realistic structure proposed in Ref. 20 and shown in Fig. 1. A unit cell of each "medium" consists of a single bilayer of two bent-arm crosses, one spiraling clockwise and the other counterclockwise. Their ordering in the z direction determines the chirality of the medium. We omit the dielectric polyimide in which the metal was embedded in Ref. 20, as this eliminates a chirality-independent attraction between the layers. The exact Casimir force between the periodic structures of Fig. 1 is computed using a finite-difference time-domain method.[13,14] Ten bilayers in the z direction are included on each side; adding more layers does not change the results. We compute the force for two different material types: perfect electric conductors (PEC) and dispersive gold. For gold we take a plasma model with $\omega_p=1.37\times10^{16}$ rad/s. The latter model requires a definite value for the length scale a, which we take to be $a=1$ μm. The results shown in Fig. 2 [each force difference is normalized by $F_{OC}(x)$] are similar for both PEC and dispersive gold and are not consistent with the EMA: even the sign of $F_{OC}(x)-F_{SC}(x)$ can be changed as a function of x for $z/a<0.75$. Larger z/a still exhibit a strong x dependence in the force.

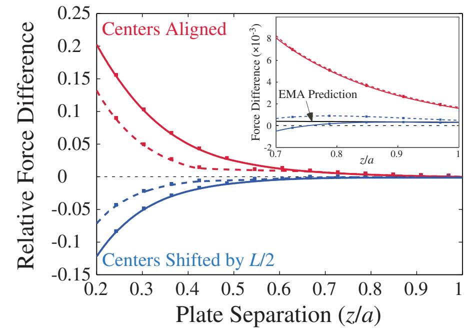

FIG. 2. (Color online) Relative force difference $(F_{OC}-F_{SC})/F_{OC}$ for the left (red) and right (blue) columns of Fig. 1 for PEC (solid) and dispersive gold for $a=1$ μm (dashed). From Fig. 1, the sign difference is due to proximity effects. The inset shows a zoom of the large-z regime, along with the EMA prediction (black).

These results for low z/a can be qualitatively described by pairwise nearest-neighbor attractions. Consider, for instance, the two cases diagrammed in Fig. 1. First, when the centers of the unit cells are aligned, there is approximately a four-bar overlap in the SC case and an eight-bar overlap in the OC case. If the force is proportional to the number of overlapping nearest-neighbor bars, we expect $F_{OC}>F_{SC}$. When the centers are displaced by $x=L/2$, SC has a four-bar overlap and OC has a three-bar overlap, so we expect $F_{OC}<F_{SC}$, and the relative force difference should be reduced by approximately 1/4. This prediction, based purely on pairwise attraction, captures the behavior for $z/a<0.75$. For larger z/a the sign of $F_{OC}-F_{SC}$ is the same in both cases, and the magnitude of the force difference is comparable to the EMA prediction. However, in this limit chiral effects are very small (accounting for only 0.1% of the force). Furthermore, as the force difference is still highly x dependent, and other transverse displacements may still switch the sign of the force difference. We therefore cannot determine if this is really an ideal chiral effect or not.

IV. OMEGA PARTICLES

As we have seen, when the chirality of the microstructure is thought to have a large effect on the force, this effect can

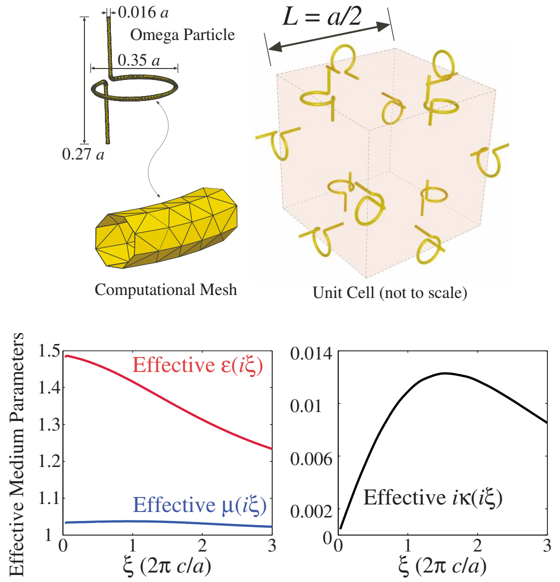

FIG. 3. (Color online) Top: unit cell of isotropic chiral metamaterial: PEC omega particles in vacuum. Shaded cube indicates relative positions in unit cell. Bottom: effective-medium parameters, as a function of imaginary frequency $\omega = i\xi$, deduced directly from imaginary-ω scattering data. $\mu(0) \neq 1$ because the particles are PEC.

actually be attributed to pairwise forces rather than chiral metamaterial effects. However, the predictions of Ref. 20 were based on *isotropic*, chiral media, and the bent-arm crosses of Fig. 1 are highly anisotropic. It is possible that the effects of this anisotropy dominate those of chirality. To obtain a chirality with minimal anisotropy, in this section we consider a more idealized system: the so-called "omega" particles,[18,20] shown in Fig. 3. Each individual particle was predicted to have a strong chiral response, and when assembled into a period-a unit cell of high symmetry should form an isotropic chiral metamaterial. The unit-cell configuration is shown in Fig. 3 (top). Figure 3 (bottom) shows the obtained EMA parameters (discussed in Sec. IV B), making this an isotropic chiral metamaterial. In fact, by picking a unit cell of lower symmetry (see below), we find that anisotropy quickly dominates chiral metamaterial effects. To make the medium as homogeneous as possible, the omega particles are relatively closely packed, and as dispersion had little qualitative role in the previous results, we take the particles to be PEC for simplicity.

A. Computational method

In this section, we outline the computational method used to compute Casimir forces between the omega particles of Fig. 3. Force computations for a structure as complex as Fig. 3 are very difficult for finite-difference methods because of the disparity of size between the periodicity a and the wire diameter $0.016a$. Instead, we employ a boundary-element formulation[12] that computes the scattering matrices of objects in imaginary ω using a nonuniform mesh of the surfaces, shown in Fig. 3. In addition, we use a dilute approximation (justified in Sec. IV C) in which multiple scattering events within a given structure are neglected, so only the scattering matrices of individual particles are required. The force between two periodic structures is then computed from the scattering matrices (see Ref. 11 for a detailed derivation, and a partial review of precursors[8–10]). The force computation is summarized as follows: first, the scattering matrix for each omega particle is numerically computed in a spherical multipole basis. This leads to a matrix of scattering amplitudes $F_{l',m',P';l,m,P}$, where l, $-l \leq m \leq l$, and l', $-l' \leq m' \leq l'$, are the respective moments of the incident and scattered spherical waves, and $P, P' \in \{M, E\}$ their polarization. Second, the scattering matrix is converted to a plane-wave basis, where for each ω the plane-wave has transverse wave vector $\mathbf{k}_\perp$ and polarization $P = s, p$. Third, to get the scattering from the unit cell of Fig. 3 we sum the scattering matrices from the twelve individual omega particles, each rotated and displaced appropriately. The rotations are applied to the spherical multipole moments via a rotation of the spherical harmonics, and the displacements are applied in the plane-wave basis via plane-wave translation matrices. Fourth, the two-dimensional periodicity of the lattice is incorporated into the problem: for scattering from a unit cell in the plane-wave basis, one computes the scattering coefficients between plane waves of arbitrary $\mathbf{k}_\perp$ and $\mathbf{k}'_\perp$, P and P'. When the scattered fields are summed over all unit cells of a periodic structure (in two dimensions), the scattering matrix gains a factor $\Sigma_{\mathbf{G}} \delta^{(2)}(\mathbf{k}_\perp - \mathbf{k}'_\perp + \mathbf{G})/a^2$, where $\{\mathbf{G}\}$ are the reciprocal lattice vectors. Therefore, only scattering between plane waves where $\mathbf{k}_\perp - \mathbf{k}'_\perp = \mathbf{G}$ are needed. Finally, to simulate a semi-infinite omega medium in z, we apply the translation matrices to the scattering amplitude of an entire unit cell, displaced by integer multiples of a in z. With this method, we can quickly compute forces for many configurations, e.g., many $x-z$ displacements. For the present computations, we find that $l \leq 3$ and $\mathbf{k}_\perp$ within the first three Brillouin zones suffice to get the force (and the force difference) to high precision.

B. Results

To demonstrate that we have an isotropic, chiral medium in the EMA, we extract the effective-medium parameters $\varepsilon(i\xi)$, $\mu(i\xi)$, and $\kappa(i\xi)$ [Fig. 3 (bottom)] from the scattering matrix at $\mathbf{k}_\perp$. Parameter retrieval[20] from reflection and transmission at normal incidence cannot be used because for imaginary ω the transmission decreases exponentially with the thickness of the medium. Instead, we compute the specular reflection coefficients $R_{ss}(\omega, \mathbf{k}_\perp)$ and $R_{sp}(\omega, \mathbf{k}_\perp)$. For each frequency $\omega = i\xi$, these quantities (given in Ref. 7) can be expanded to quadratic order in $|k_\perp| \ll \xi$ and κ. The coefficients of each term are determined by a fit (with $|\mathbf{k}_\perp| < \xi/10$).

The results of the force computations are shown in Fig. 4 and are similar in form to Fig. 2. We examine the relative force difference at each z/a—normalizing by the minimum force is convenient to obtain a positive difference that can be plotted on a log scale. The shaded areas of each color represent the range of values that the force assumes for all transverse (x) displacements. Their spread (the x dependence) in-

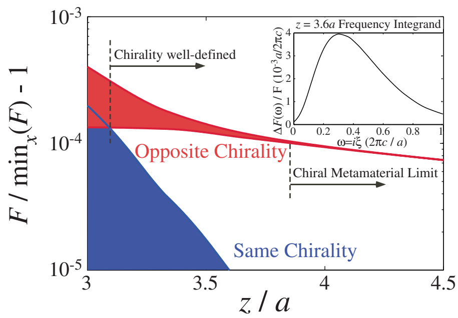

FIG. 4. (Color online) Forces (in dilute approximation) between chiral media from Fig. 3 for the SC (blue) and OC (red) cases. The range of the force across all transverse (x) displacements is shaded and normalized by the minimum of the force over all x. For $z \lesssim 3.1a$, chirality is not well defined (curves overlap). Only when curves are distinct and x independent can the systems be described as chiral metamaterials. Inset: frequency integrand of the relative force difference at $z=3.6a$. The smallness of the $\omega=0$ term is an indicator that this difference is due to chirality and not anisotropy (see text).

dicates breakdown of the EMA, and for $z \lesssim 3.1a$ it is so severe that the red and blue force curves overlap. When these curves separate, but before they sharpen [the blue (SC) curve goes to zero], we have an intermediate regime where chiral effects are competing with proximity effects. Only when the curve thickness is much less than the relative force difference ($\lesssim 10\%$ for $z \gtrsim 3.6a$) is EMA accurate. As mentioned above, we designed the unit cell to be highly isotropic, for which the EMA parameters ε, μ, κ are truly scalars. For a less isotropic unit cell (e.g., only one omega particle per unit cell), the relative force difference can be made much larger, but the source of this difference is ambiguous, as in Fig. 2. For two purely chiral materials in the EMA regime, the zero-frequency component of the force difference is exactly zero[7] so the magnitude of the zero-frequency component is an indication of whether the force difference arises from chirality alone. In Fig. 4 (inset) we display the frequency integrand at $z=3.6a$, indicating that the force difference in the isotropic case is indeed due to chirality. However, we have found that the frequency integrand for less isotropic unit cells has a large zero-frequency component, indicating that anisotropy and proximity effects play a large role in that case. This could also explain the results of Fig. 2 for larger z.

C. Dilute approximation

We now comment on the validity of the effective-medium picture and the dilute approximation. One can compute the Casimir force and the force difference from the EMA parameters of Fig. 3. For the range of z/a in Fig. 4, this gives the correct force between the two media but overestimates the force difference by roughly 30%. This is because the error terms in the EMA above are $O(k_\perp^4)$, the same order as the chirality contributions $\sim R_{\mathrm{sp}}^2$ to the force.[7] The Clausius-Mossotti (C-M) equation allows us to check the validity of the dilute approximation. C-M relates polarizabilities of particles to the effective-medium parameters.[18,21] We compute the polarizabilities from C-M, working backward from the effective-medium parameters of Fig. 3 (expanding C-M to first order in the polarizability), and plug this into the full C-M to compute the nondilute correction. The relative force difference of Fig. 4 is changed by $<15\%$. C-M is obtained in the static limit, whereas at finite imaginary ω the exponential field decay reduces the interactions, so this is an overestimate.

V. CONCLUSIONS

Based on numerical calculations involving the exact microstructure of possible chiral metamaterials, we find that to observe an unambiguous effect of chirality in isotropic, chiral metamaterials, one must measure the total force to four digits of accuracy. Given that it is controversial whether even 1% accuracy can be obtained in Casimir measurements for simple geometries,[22] combined with the restrictions on length scales that are imposed by the need to fabricate a complex microstructure, detecting such a 10^{-4} effect appears virtually impossible. Although these calculations are for specific metamaterial structures, they are for two of the most promising known chiral structures, for idealized perfect metals, and moreover we find that two radically different structures yield similarly small chiral effects. While this does not preclude the possibility of observing other interesting Casimir effects in metamaterials (especially if they rely on the $\omega \rightarrow 0$ response of the metamaterial), it suggests serious limitations for finite-ω effects. Further, this analysis highlights the importance of accounting for the exact microstructures involved, as they can have an important effect on the conclusions reached.

ACKNOWLEDGMENTS

We thank P. Bermel and S. J. Rahi for useful discussions. This work was supported by the Army Research Office through the ISN under Contract No. W911NF-07-D-0004 and by DARPA under Contract No. N66001-09-1-2070-DOD and under DOE/NNSA through Contract No. DE-AC52-06NA25396.

[1] C. Henkel and K. Joulain, Europhys. Lett. **72**, 929 (2005).
[2] U. Leonhardt and T. G. Philbin, New J. Phys. **9**, 254 (2007).
[3] F. S. S. Rosa, D. A. R. Dalvit, and P. W. Milonni, Phys. Rev. Lett. **100**, 183602 (2008).
[4] M. G. Silveirinha and S. I. Maslovski, arXiv:1007.1582 (unpublished).
[5] S. J. Rahi, M. Kardar, and T. Emig, Phys. Rev. Lett. **105**, 070404 (2010).
[6] M. Levin, A. P. McCauley, A. W. Rodriguez, M. T. Homer Reid,

and S. G. Johnson, Phys. Rev. Lett. **105**, 090403 (2010).
[7] R. Zhao, J. Zhou, T. Koschny, E. N. Economou, and C. M. Soukoulis, Phys. Rev. Lett. **103**, 103602 (2009).
[8] T. Emig, N. Graham, R. L. Jaffe, and M. Kardar, Phys. Rev. Lett. **99**, 170403 (2007).
[9] O. Kenneth and I. Klich, Phys. Rev. B **78**, 014103 (2008).
[10] P. A. Maia Neto, A. Lambrecht, and S. Reynaud, Phys. Rev. A **78**, 012115 (2008).
[11] S. J. Rahi, T. Emig, N. Graham, R. L. Jaffe, and M. Kardar, Phys. Rev. D **80**, 085021 (2009).
[12] M. T. Homer Reid, A. W. Rodriguez, J. White, and S. G. Johnson, Phys. Rev. Lett. **103**, 040401 (2009).
[13] A. W. Rodriguez, A. P. McCauley, J. D. Joannopoulos, and S. G. Johnson, Phys. Rev. A **80**, 012115 (2009).
[14] A. P. McCauley, A. W. Rodriguez, J. D. Joannopoulos, and S. G. Johnson, Phys. Rev. A **81**, 012119 (2010).
[15] L. D. Landau, E. M. Lifshitz, and L. P. Pitaevskiĭ, *Statistical Physics Part 2* (Pergamon, Oxford, 1960), Vol. 9.
[16] O. Kenneth, I. Klich, A. Mann, and M. Revzen, Phys. Rev. Lett. **89**, 033001 (2002).
[17] F. S. S. Rosa, J. Phys.: Conf. Ser. **161**, 012039 (2009).
[18] S. Tretyakov, A. Shivola, and L. Jylha, Photonics Nanostruct. Fundam. Appl. **3**, 107 (2005).
[19] B. V. Derjaguin, I. I. Abrikosova, and E. M. Lifshitz, Q. Rev., Chem. Soc. **10**, 295 (1956).
[20] R. Zhao, T. Koschny, E. N. Economou, and C. M. Soukoulis, Phys. Rev. B **81**, 235126 (2010).
[21] R. E. Collin, *Field Theory of Guided Waves*, 2nd ed. (IEEE Press, New York, NY, 1991).
[22] S. Lamoreaux, arXiv:1008.3640 (unpublished).